

A STUDY OF CORRELATIONS BETWEEN IDENTIFIED CHARGED HADRONS IN HADRONIC Z^0 DECAYS*

The SLD Collaboration**

Stanford Linear Accelerator Center

Stanford University, Stanford, CA 94309

ABSTRACT

We present a preliminary study of correlations in rapidity between pairs of identified pions, kaons and protons in hadronic Z^0 decays into light flavors. Short range charge correlations are observed between all combinations of these hadron species, confirming that charge, strangeness and baryon number are conserved locally in the jet fragmentation process. The range of this effect is found to be independent of momentum. A strong long-range correlation is observed for high-momentum charged kaon pairs, and weaker long-range $\pi^+ - \pi^-$, $\pi^+ - K^-$ and $p - K^-$ correlations are observed. The SLC electron beam polarization is used to tag the quark hemisphere in each event, allowing the first study of rapidities signed such that positive rapidity is along the quark rather than antiquark direction. Distributions of signed rapidities and of ordered differences between signed rapidities provide new insights into leading particle production and several new tests of fragmentation models.

Contributed to the XXIX International Conference on High Energy Physics, Vancouver, B.C. Canada, July 23-29 1998: parallel session 3; plenary sessions 4, 18.

*Work supported by Department of Energy contract DE-AC03-76SF00515.

1 Introduction

Correlations between particles produced in hadronic jets can be used to probe details of the jet fragmentation process. In e^+e^- annihilations into hadrons, the total charge, strangeness, baryon number, etc. of the final state particles in each event must be zero, and it is interesting to ask whether the conservation of such quantum numbers is local, or is longer-range in character. For example, in the case of strangeness, one can ask whether a strange particle and a corresponding antistrange particle tend to be produced “close” to each other within the event, whether strange and antistrange particles are associated with the initial \bar{s} and s quarks, respectively, in $s\bar{s}$ events (or with the initial u and \bar{u} in $u\bar{u}$ events, etc.), or whether strange and antistrange particles are distributed randomly throughout the event. Similar questions can be posed for other relevant quantum numbers. Previous studies [1] of differences in rapidity between associated identified hadrons have shown that the conservation of charge, strangeness and baryon number is predominantly local. Most fragmentation models implicitly implement this feature, and the form and range of such short-range correlations provide useful tests of these models. Short-range correlations can also arise from the decays of heavier hadrons, for example the decay $\rho^0 \rightarrow \pi^+\pi^-$ will produce opposite-charge pion pairs with a characteristic degree of locality.

Long-range correlations between particles of opposite charge and strangeness in opposite jets of an event have also been observed [2]. These can be understood in terms of leading particle production whereby the higher-rapidity tracks in each jet tend to carry the quantum numbers of the initial quark or antiquark. In the case of $e^+e^- \rightarrow s\bar{s}$ events, the s and \bar{s} quarks may hadronize into a high momentum K^- and K^+ , respectively, and there need be no other strange particles in the event. In $u\bar{u}$ and $d\bar{d}$ events, however, the locality of quantum number conservation implies that a high-momentum strange-antistrange, baryon-antibaryon, etc. *pair* must be produced in each jet, which will dilute any long-range correlation. Nevertheless, improved measurements of long-range correlations may provide better understanding of leading particle production.

The rapidity of a particle is typically defined with an arbitrary sign. If a sign could be given to each measured rapidity such that, for example, positive (negative) rapidity corresponds to the initial quark (antiquark) direction, then one might probe more deeply into both leading and nonleading particle production. One could measure, for

example, the extent to which a leading particle has higher rapidity than its associated antiparticle, and the extent to which low-momentum particles in jets remember the initial quark/antiquark direction.

In this paper we present a study of correlations in rapidity between identified charged pions, kaons and protons based on about 300,000 hadronic Z^0 decays recorded by the SLD experiment at the SLAC Linear Collider. Clean samples of identified particles were obtained using the Cherenkov Ring Imaging Detector. Light-flavor events ($e^+e^- \rightarrow u\bar{u}, d\bar{d}$ or $s\bar{s}$) were selected in order to remove the effects of the decays of the leading bottom and charmed hadrons in heavy flavor events. In section 4 we present a study of short-range correlations between all pairs of these hadron species as a function of hadron momentum. We quantify the range of each correlation, and compare with the predictions of the JETSET fragmentation model. In section 5 we search for long-range correlations between these species. In section 6 we exploit the SLC electron beam polarization to identify the quark (vs. antiquark) hemisphere in each event and sign the rapidities such that particles in the quark-tagged hemisphere have positive rapidity. We interpret the signed rapidity distributions themselves in terms of leading particle effects, and use rapidity differences between particle pairs to probe more deeply into this topic.

2 Apparatus and Hadronic Event Selection

A general description of the SLD can be found elsewhere [3]. The trigger and initial selection criteria for hadronic Z^0 decays are described in Ref. [4]. This analysis used charged tracks measured in the Central Drift Chamber (CDC) [5] and Vertex Detector (VXD) [6], and identified using the Cherenkov Ring Imaging Detector (CRID) [7]. Momentum measurement is provided by a uniform axial magnetic field of 0.6T. The CDC and VXD give a momentum resolution of $\sigma_{p_\perp}/p_\perp = 0.01 \oplus 0.0026p_\perp$, where p_\perp is the track momentum transverse to the beam axis in GeV/c. One half of the data were taken with the original vertex detector (VXD2), and the other half with the upgraded detector (VXD3). In the plane normal to the beamline the centroid of the micron-sized SLC IP was reconstructed from tracks in sets of approximately thirty sequential hadronic Z^0 decays to a precision of $\sigma_{IP} \simeq 7 \mu\text{m}$ for the VXD2 data and $\simeq 5$

μm for the VXD3 data. Including the uncertainty on the IP position, the resolution on the charged track impact parameter (d) projected in the plane perpendicular to the beamline is $\sigma_d = 11 \oplus 70 / (p_{\perp} \sin^{3/2} \theta)$ μm for VXD2 and $\sigma_d = 9 \oplus 29 / (p_{\perp} \sin^{3/2} \theta)$ μm for VXD3, where θ is the track polar angle with respect to the beamline. The CRID comprises two radiator systems that between them identify charged pions with high efficiency and purity in the momentum range 0.3–35 GeV/c, charged kaons in the ranges 0.75–6 GeV/c and 9–35 GeV/c, and protons in the ranges 0.75–6 GeV/c and 10–46 GeV/c [8]. The event thrust axis [9] was calculated using energy clusters measured in the Liquid Argon Calorimeter [10].

A set of cuts was applied to the data to select well-measured tracks and events well contained within the detector acceptance. Charged tracks were required to have a distance of closest approach transverse to the beam axis within 5 cm, and within 10 cm along the axis from the measured IP, as well as $|\cos \theta| < 0.80$, and $p_{\perp} > 0.15$ GeV/c. Events were required to have a minimum of seven such tracks, a thrust axis polar angle w.r.t. the beamline, θ_T , within $|\cos \theta_T| < 0.71$, and a charged visible energy E_{vis} of at least 20 GeV, which was calculated from the selected tracks assigned the charged pion mass. The efficiency for selecting a well-contained $Z^0 \rightarrow q\bar{q}(g)$ event was estimated to be above 96% independent of quark flavor.

In order to reduce the effects of decays of heavy hadrons, we selected light-flavor events ($u\bar{u}$, $d\bar{d}$ and $s\bar{s}$) by requiring all tracks in the event with high quality [11] to have a transverse impact parameter with respect to the IP of less than three times its estimated error. Finally, the CRID was required to be operational. The selected sample comprised roughly 94,000 events, with an estimated background of 13% from $c\bar{c}$ events, 1% from $b\bar{b}$ events, and a non-hadronic background contribution of $0.10 \pm 0.05\%$ dominated by $Z^0 \rightarrow \tau^+\tau^-$ events.

For the purpose of estimating the efficiency and purity of the event flavor tagging and the particle identification, we made use of a detailed Monte Carlo (MC) simulation of the detector. The JETSET 7.4 [12] event generator was used, with parameter values tuned to hadronic e^+e^- annihilation data [13], combined with a simulation of B -hadron decays tuned [14] to $\Upsilon(4S)$ data and a simulation of the SLD based on GEANT 3.21 [15]. Inclusive distributions of single-particle and event-topology observables in hadronic events were found to be well described by the simulation [4].

3 Identified Particle Selection

The identification of charged tracks as pions, kaons or protons using the CRID is described in detail in [8]. For this analysis we used a relatively loose identification algorithm, since the presence of misidentified hadrons at the 10% level has little effect on the measured correlations. Tracks with poor CRID information or that were likely to have scattered or interacted before exiting the CRID were removed by requiring each track to have at least 40 CDC hits, at least one of which was at a radius of at least 92 cm, to extrapolate through an active region of the appropriate CRID radiator and through a live CRID TPC, and, in the case of the gas radiator, to have fewer than four saturated hits within the volume in which the gas ring is expected. Approximately 85% of the tracks within the CRID acceptance satisfied these cuts.

Tracks identified in the calorimeters as electrons or muons [16] were rejected, and for the remaining tracks log-likelihoods [8, 17] were calculated for each of the three charged hadron hypotheses $i = \pi, K$ and p , and for each of the liquid and gas radiators. A track was tagged as a hadron of species i by the liquid (gas) system if the log-likelihood for hypothesis i exceeded both of the other log-likelihoods by at least 5 (3) units. In addition, for those tracks with good information from both the liquid and gas systems, the liquid and gas log-likelihoods were added together, and a track was tagged by the combined system if the log-likelihood for hypothesis i exceeded both of the others by at least 3 units. A track was identified as an i -hadron if it was tagged as type i by any of the liquid, gas or combined systems, and it was not tagged as any other type by any other system. The efficiencies for identifying accepted tracks are similar to those given in [8]: for charged pions there is roughly constant efficiency of about 80% in the momentum range 0.5–25 GeV/c; charged kaons and protons have similar efficiency except for a dip in the range 5–10 GeV/c. The simulation was found to provide a good description of the momentum distributions of the identified hadrons.

For each identified track the rapidity $y = 0.5 \ln((E + p_{\parallel})/(E - p_{\parallel}))$ was calculated using the measured momentum and its projection p_{\parallel} along the thrust axis, and the appropriate hadron mass. The distributions of rapidity are shown in fig. 1 for each identified hadron sample, along with prediction of the simulation. Note that the overall sign of the thrust axis vector, and therefore the sign of the rapidity, is arbitrary. These distributions are not flat in the central region, but show structure due to the

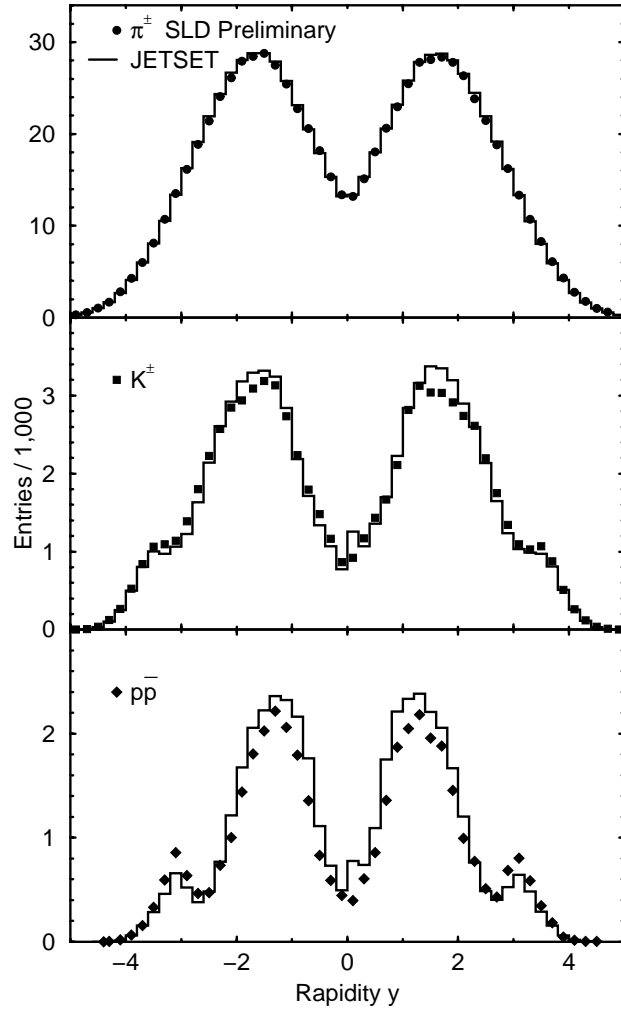


Figure 1: Rapidity distributions for the identified pions, kaons and protons. Also shown are the prediction of the Monte Carlo simulation.

momentum dependence of the CRID identification efficiency (see [8]). The simulation provides a good qualitative description of the rapidity distributions, and indicates that the dependence of the identification efficiency on momentum has only modest effects on the correlation studies, as discussed below.

The absolute value of the difference between the rapidities of each pair of identified tracks was calculated, and the distribution of this quantity is shown in fig. 2 for each of the six possible pairs of hadron types. In each case the distribution for those pairs with opposite charge is shown as the solid histogram and that for pairs with the same charge is shown as the dotted histogram.

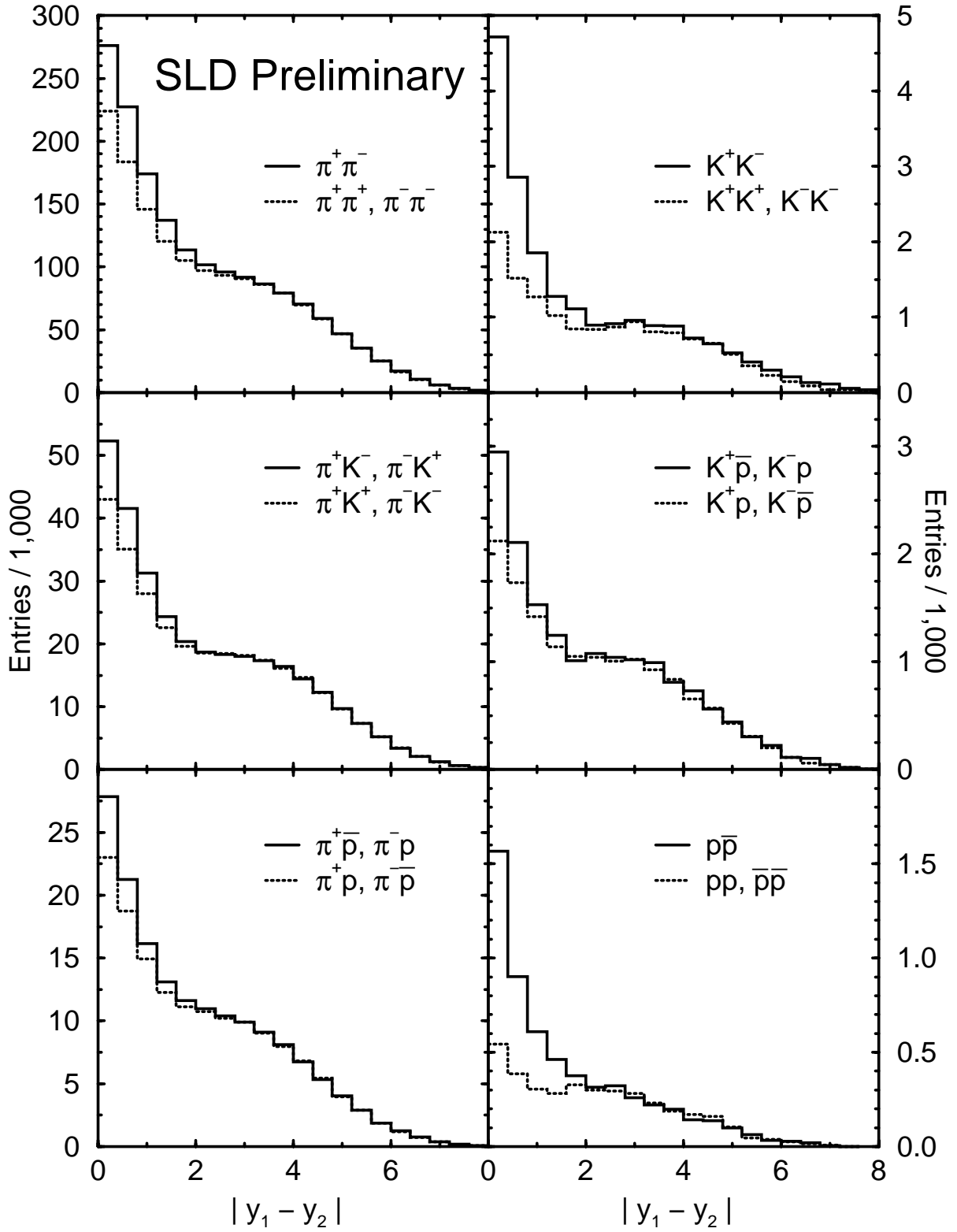


Figure 2: Rapidity difference distributions for opposite-charge (histograms) and same-charge (dashed histograms) pairs of identified pions, kaons and protons.

4 Short-Range Correlations

For every type of hadron pair in fig. 2 there is an excess of opposite-charge pairs over same-charge pairs at small values of the absolute rapidity difference $|\Delta y| = |y_1 - y_2|$. In the case of KK and pp pairs, as well as for the sum of all charged tracks, we expect more opposite-charge pairs than same-charge pairs due to conservation of strangeness, baryon number and electric charge, respectively. In the case of KK (pp) pairs the size of the excess is sensitive to the relative fraction of strange-antistrange (baryon-antibaryon) pairs that are both charged rather than neutral; if e.g. $p-\bar{n}$ were the only type of baryon-antibaryon pair produce, there would be no such excess.

The fact that the excess of opposite-charge KK and pp pairs peaks at low values of $|\Delta y|$ indicates that conservation of strangeness and baryon number, respectively, is local, as has been observed previously [1]. The similar excesses at short range for the other types of pairs indicate local conservation of electric charge and suggests that there is charge ordering among hadrons of all types in the fragmentation process.

In order to study these short-range correlations in more detail, we assumed that all same-charge pairs are unassociated, and subtracted their $|\Delta y|$ distributions from those of the respective opposite-charge pairs. These differences are shown for the low $|\Delta y|$ region in fig. 3, and are seen to differ significantly from each other in shape. Monte Carlo studies indicate that these differences are not due to acceptance, momentum dependence of the particle identification efficiency or to background from misidentified particles. Also shown in fig. 3 are the predictions of the simulation for this difference. In all cases, the simulation gives a reasonable description of the shape of the difference, although there are is a significant normalization difference for pp pairs and differences in details of the shape for $\pi\pi$, KK and πp pairs. The simulated distributions for those pairs in which both tracks are not decay products of the same heavier particle are also shown. The effect of decays on the size and shape of the difference is large for $\pi\pi$, πK , πp and KK pairs.

We have studied these short-range correlations in 6 bins of the momentum of the heavier (higher momentum) particle in the case of πK , πp and Kp ($\pi\pi$, KK and pp) pairs. We find the quality of the simulated description of the data to be independent of the momentum bin.

In order to quantify the range of each correlation, we fitted an ad hoc function,

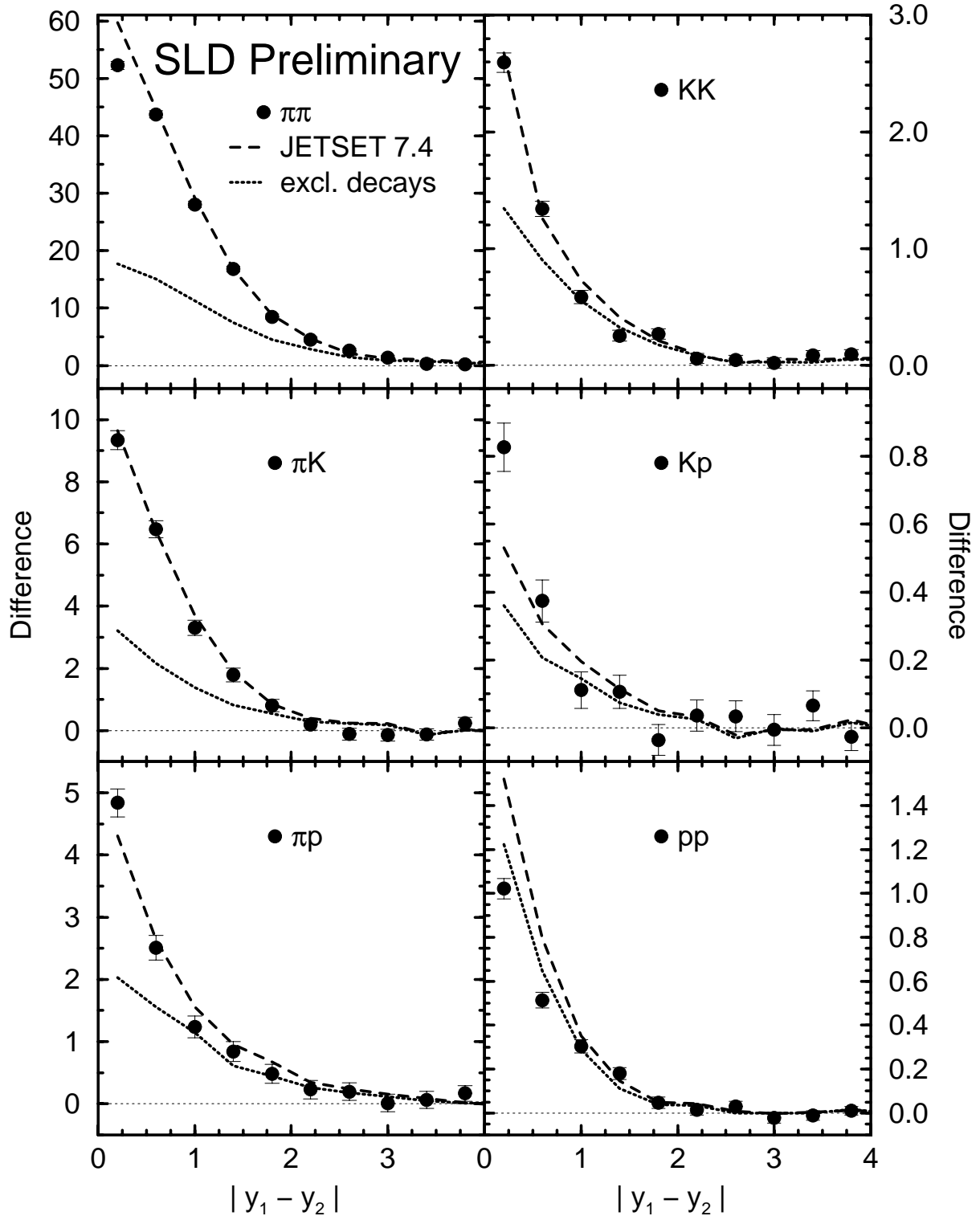


Figure 3: Differences between the $|\Delta y|$ distributions for opposite-charge and same-charge pairs in the small $|\Delta y|$ region. Also shown are the predictions of the Monte Carlo simulation for all detected pairs (dashed lines) and those pairs that are not products of the decay of the same particle (dotted lines).

the sum of two Gaussians, to each difference over the range $0 < |\Delta y| < 3$ units. The centers of both Gaussians were fixed to zero, and the amplitude (width) of the wider Gaussian was fixed to 0.4 (2.2) times that of the narrower Gaussian, leaving the amplitude and width of the narrower Gaussian as free parameters. We used the width as a measure of the range of the correlation. This function provided a reasonable qualitative description of the data for all pair types in all momentum bins, although a number of fits had poor χ^2 . The fitted widths are shown in fig. 4 as a function of momentum for each pair type. If the fragmentation process is scale invariant, then we expect the range to be independent of momentum, except for biases introduced by the bin edges and the particle identification. In the case of $\pi\pi$, the range is constant within a few percent except for the highest momentum bin. Significant momentum dependence is observed for KK , Kp and pp , however this dependence is reproduced by the simulation, with the possible exception of a difference in slope for Kp pairs. In the simulation, there is a small, smooth, parabolic momentum dependence due to binning and particle decays. The slopes and point-to-point structure are due to the momentum dependence of the particle identification efficiencies. We therefore conclude that, within the context of the JETSET model, the range of the short-range rapidity correlation for a given pair type is independent of momentum.

5 Long-Range Correlations

We next searched for long-range correlations between all types of pairs. In fig. 2 a difference between opposite-charge and same-charge pairs at high $|\Delta y|$ is visible only in the case of KK , and even here the background from uncorrelated pairs is dominant. Figure 5 shows the differences between opposite-charge and same-charge $|\Delta y|$ distributions in the high- $|\Delta y|$ region with an expanded vertical scale. A clear long-range correlation is visible for KK pairs for $|\Delta y| > 4$ and significant long-range correlations are also observed for $\pi\pi$ pairs. The predictions of the simulation are consistent with these observations, and the simulation predicts small correlations for πp and pp pairs, as well as an anticorrelation for πK pairs, however our data are not sufficiently precise to distinguish these predictions from zero.

Since we expect long-range correlations from leading particle production to be rel-

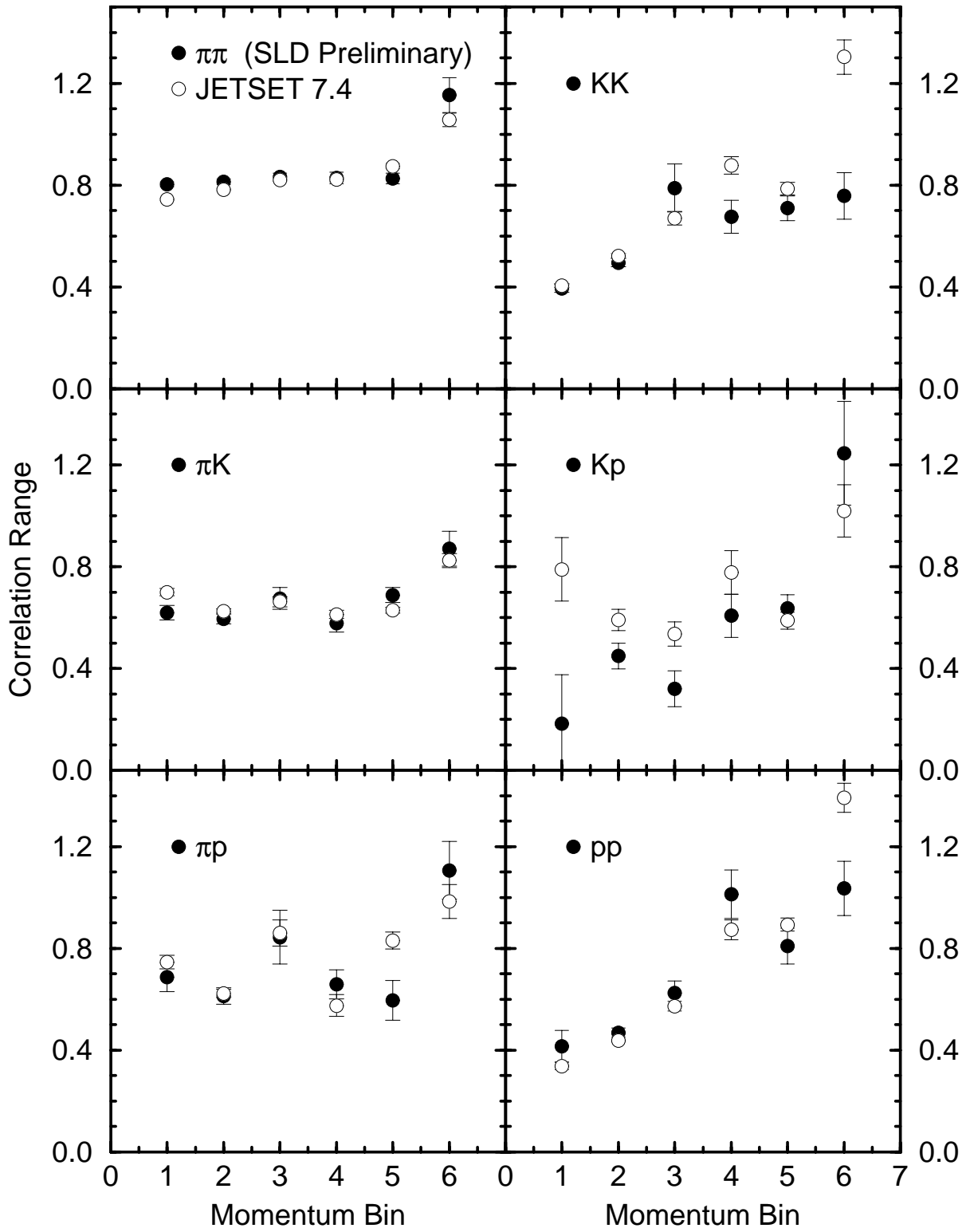


Figure 4: Range (see text) of the short-range correlations in six bins of momentum.

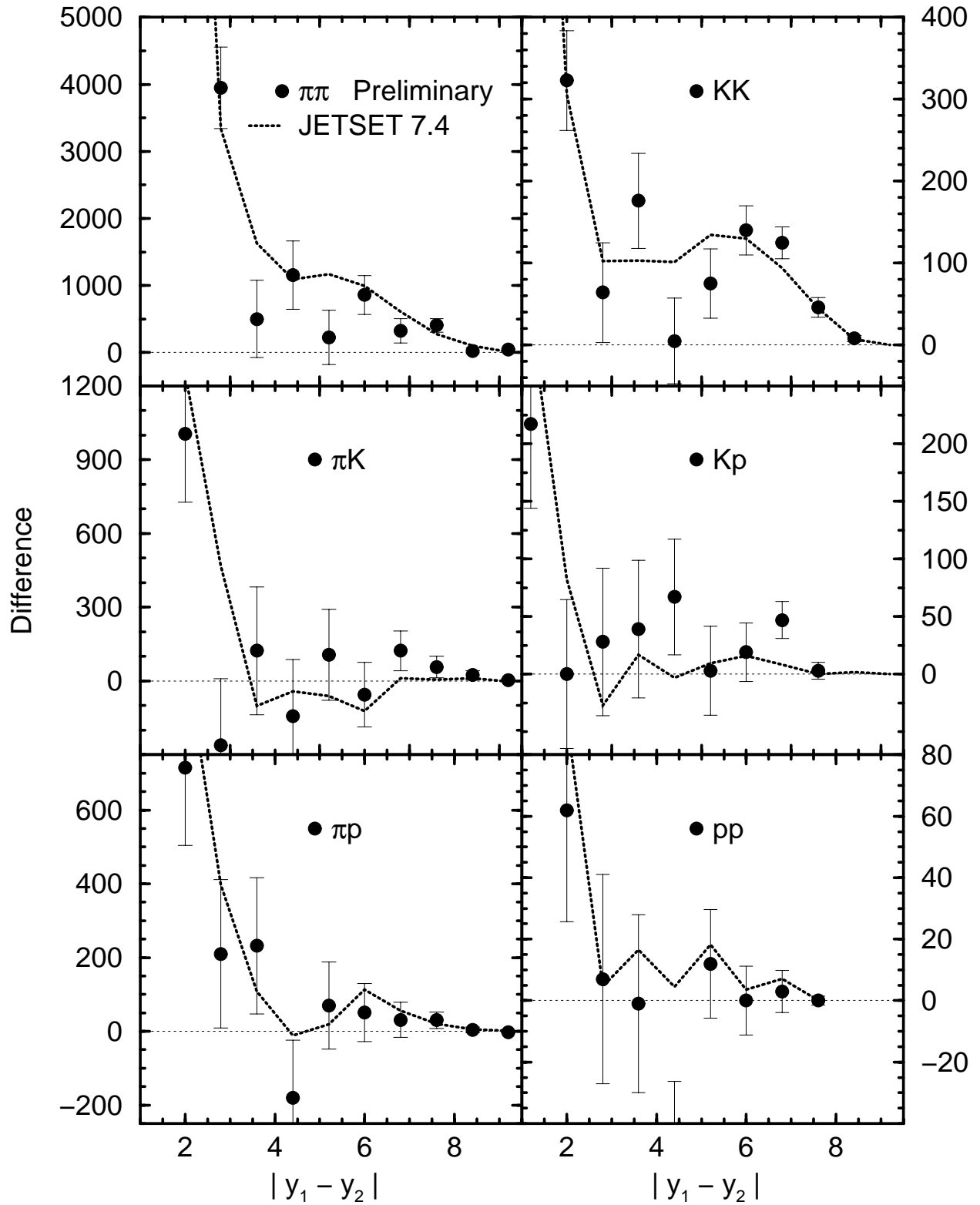


Figure 5: Differences between the $|\Delta y|$ distributions for opposite-charge and same-charge pairs in the high $|\Delta y|$ region. Also shown are the prediction of the Monte Carlo simulation.

atively more important at high momentum, we have studied these differences as a function of momentum. Figure 6 shows the differences at high $|\Delta y|$ for KK pairs in each of our six momentum bins. There is no significant correlation for $p < 9$ GeV/c, and the correlation becomes progressively more significant in the three higher momentum bins. Similar behaviour is observed for $\pi\pi$ pairs (not shown). The simulation gives a good description of this behaviour in both cases.

Imposing the requirement that both tracks in the pair have momentum $p > 9$ GeV/c results in the $|\Delta y|$ distributions shown in fig. 7. For these high-momentum pairs, there is a clear separation between pairs in the same jet ($|\Delta y| < 2.5$) and those in opposite jets ($|\Delta y| > 4$). At short range there is a large excess of opposite-charge pairs over same-charge pairs for all pair types, confirming that locality holds even at the highest momenta. At long range, there are clear correlations visible for $\pi\pi$, πK , KK and Kp . The total numbers of entries in each distribution for $|\Delta y| > 4$ are given in table 1, along with the differences between the numbers of opposite-charge and same-charge pairs of each type. The predictions of the simulation are also given and the total numbers predicted are generally consistent with the data, except that the simulation predicts much smaller πK and Kp correlations than are observed in the data, and a larger $\pi\pi$ correlation.

6 Signed Rapidities and Correlations

We next tagged the quark (vs. antiquark) direction in each hadronic event using the electron beam polarization for that event, exploiting the large forward-backward quark production asymmetry in Z^0 decays. If the beam was left-(right-)handed then the thrust axis was signed such that $\cos \theta_T$ was positive (negative). Events with $|\cos \theta_T| < 0.15$ were removed, as the production asymmetry is small in this region. The probability to tag the quark direction correctly in these events was 73%.

The rapidity of a particle with respect to the signed thrust axis is naturally signed such that positive rapidity corresponds to the hemisphere in the tagged direction of the initial quark, and negative rapidity corresponds to the tagged antiquark hemisphere. The signed rapidity distributions for identified K^+ and K^- are shown in fig. 8. There is a clear difference between the two, with more K^- than K^+ in the quark hemisphere, as

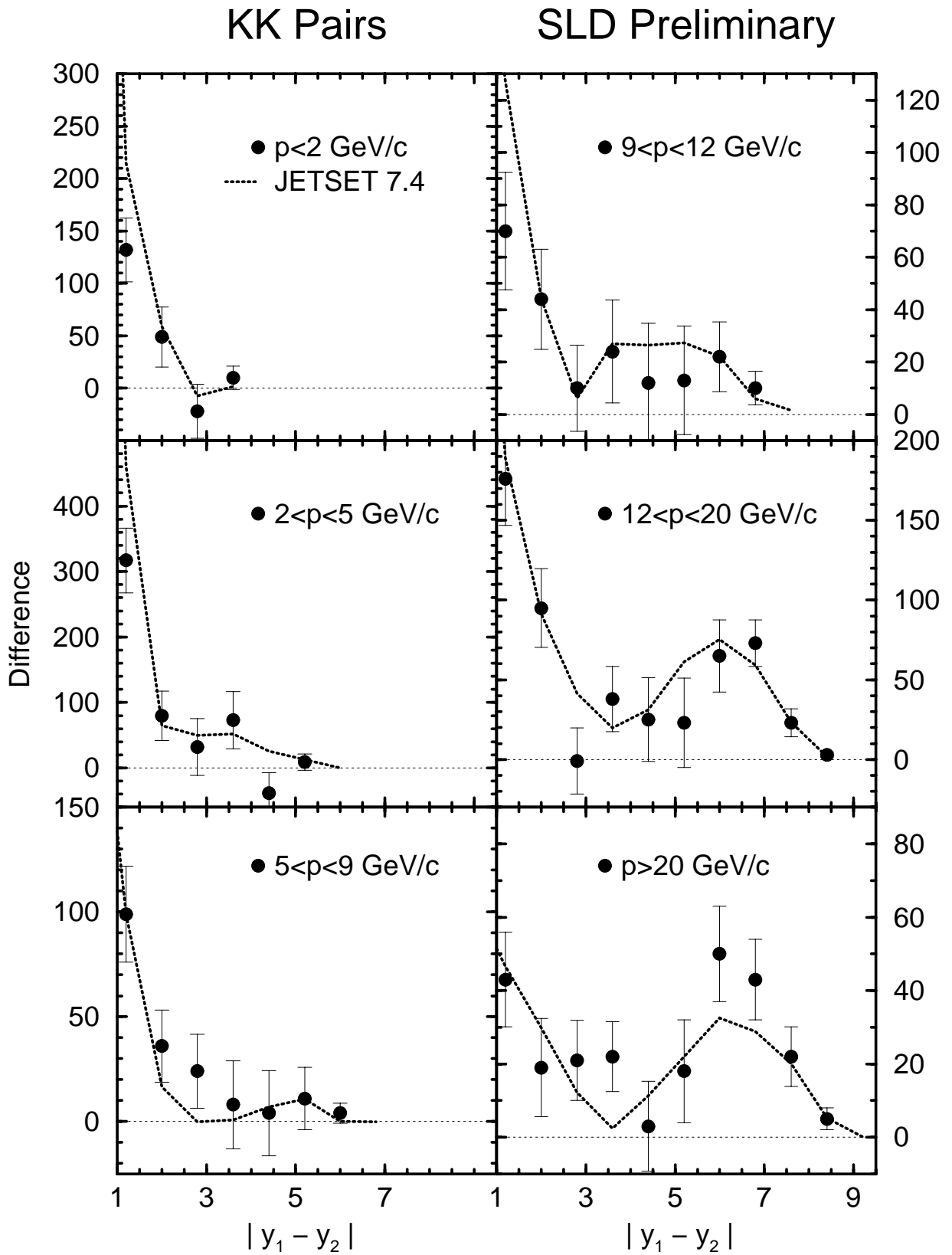


Figure 6: Differences between the $|\Delta y|$ distributions for opposite-charge and same-charge kaon pairs in six bins of the momentum of the higher-momentum kaon. Also shown are the prediction of the Monte Carlo simulation.

Momentum > 9 GeV/c for both tracks

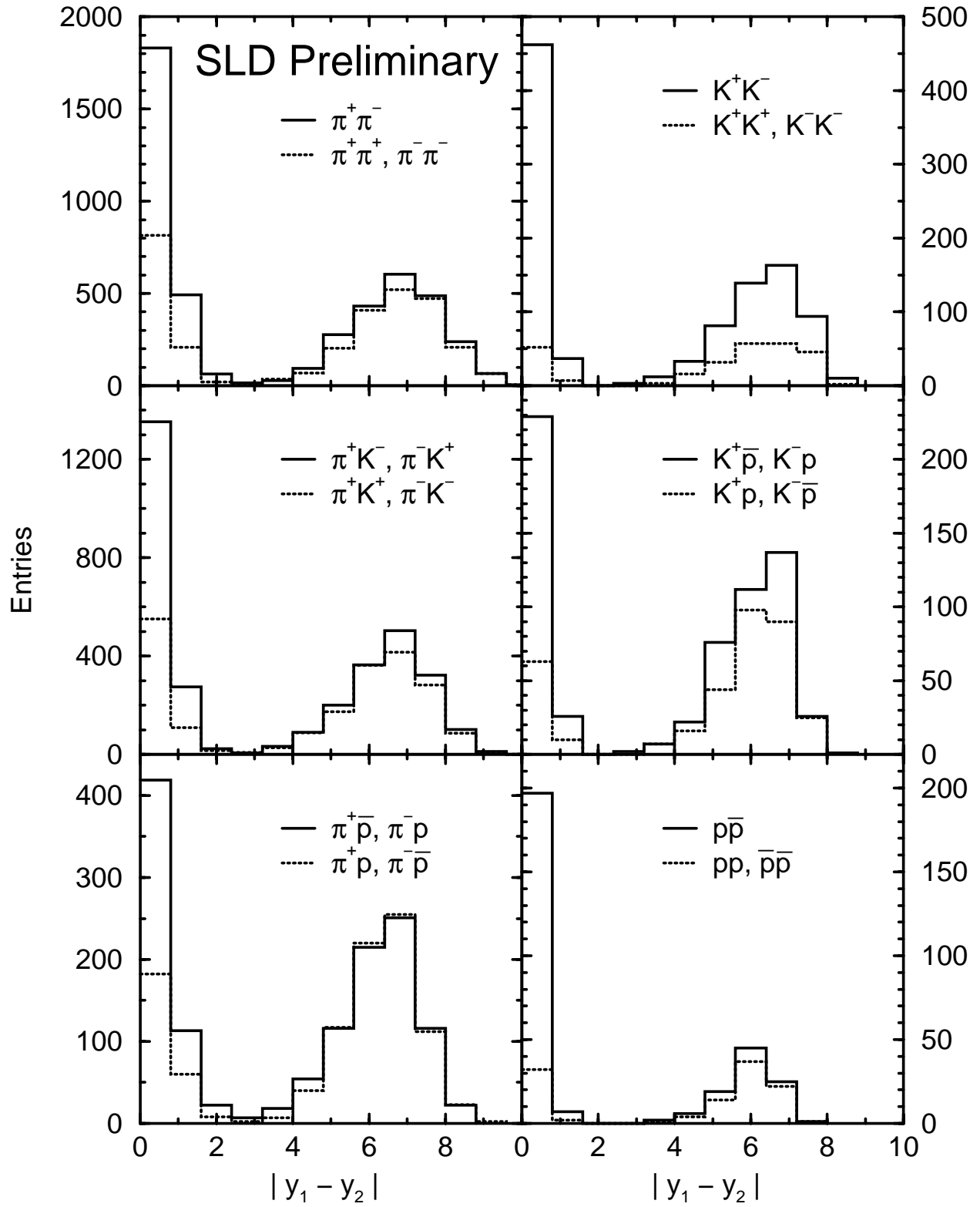


Figure 7: $|\Delta y|$ distributions for opposite-charge (histograms) and same-charge (dashed histograms) pairs in which both tracks have momentum greater than 9 GeV/c.

Pair Type	Data			Simulation		
	Opposite Charge	Same Charge	Difference	Opposite Charge	Same Charge	Difference
$\pi\pi$	2208	1955	253 ± 64	2339	2038	301 ± 29
πK	1597	1421	176 ± 55	1432	1414	18 ± 23
πp	774	769	5 ± 40	772	687	85 ± 17
KK	520	210	310 ± 25	491	225	266 ± 11
Kp	374	273	101 ± 25	290	249	40 ± 10
pp	96	78	18 ± 13	67	55	12 ± 05

Table 1: Observed numbers of opposite-charge and same-charge pairs in which both tracks had $p > 9$ GeV/c and the $|\Delta y| > 4$, and the difference between the number of opposite-charge and same-charge pairs. Also shown are the predictions of the Monte Carlo simulation.

expected due to leading K^- produced in s quark jets [8, 18]. The difference between the two distributions is also shown in the figure and is compared with the MC prediction, which is consistent with the data.

Figure 9 shows similar distributions for all three identified particle types for tracks with momenta above 9 GeV/c. In this case the differences at negative Δy have been subtracted from those at positive Δy for optimal use of the data sample. The large differences between the signed rapidity distributions for K^- and K^+ and for p and \bar{p} confirm our previous observation [18] of substantial leading kaon and baryon production in light quark jets. There is also a significant difference between π^+ and π^- , which, along with the above observation of a long-range $\pi\pi$ correlation, provides direct evidence for leading pion production. The difference is negative, which is expected if leading pions are produced equally in u and d jets, since $d\bar{d}$ events are more plentiful than $u\bar{u}$ events in Z^0 decays. The predictions of the simulation are consistent with the $\pi\pi$ and KK data, but underestimate the difference for pp pairs.

For pairs of identified particles, one can define an ordered rapidity difference. For particle-antiparticle pairs, we define $\Delta y^{+-} = y_+ - y_-$ as the difference between the signed rapidities of the positively charged particle and the negatively charged parti-

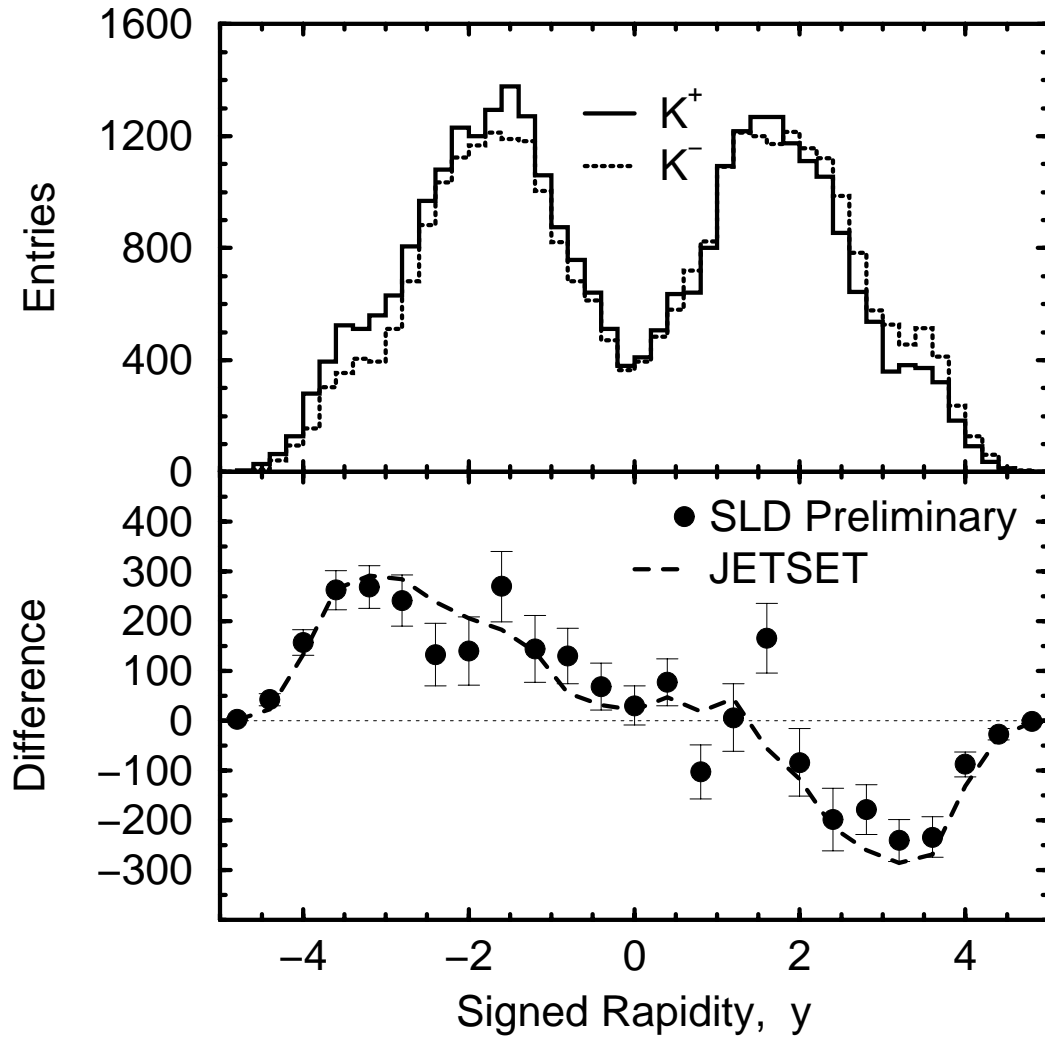


Figure 8: Distributions (top) of the rapidity with respect to the signed thrust axis for positively (histogram) and negatively (dashed histograms) charged kaons. The difference (bottom) between these two distributions compared with the prediction of the Monte Carlo simulation.

Tracks with $p > 9 \text{ GeV}/c$

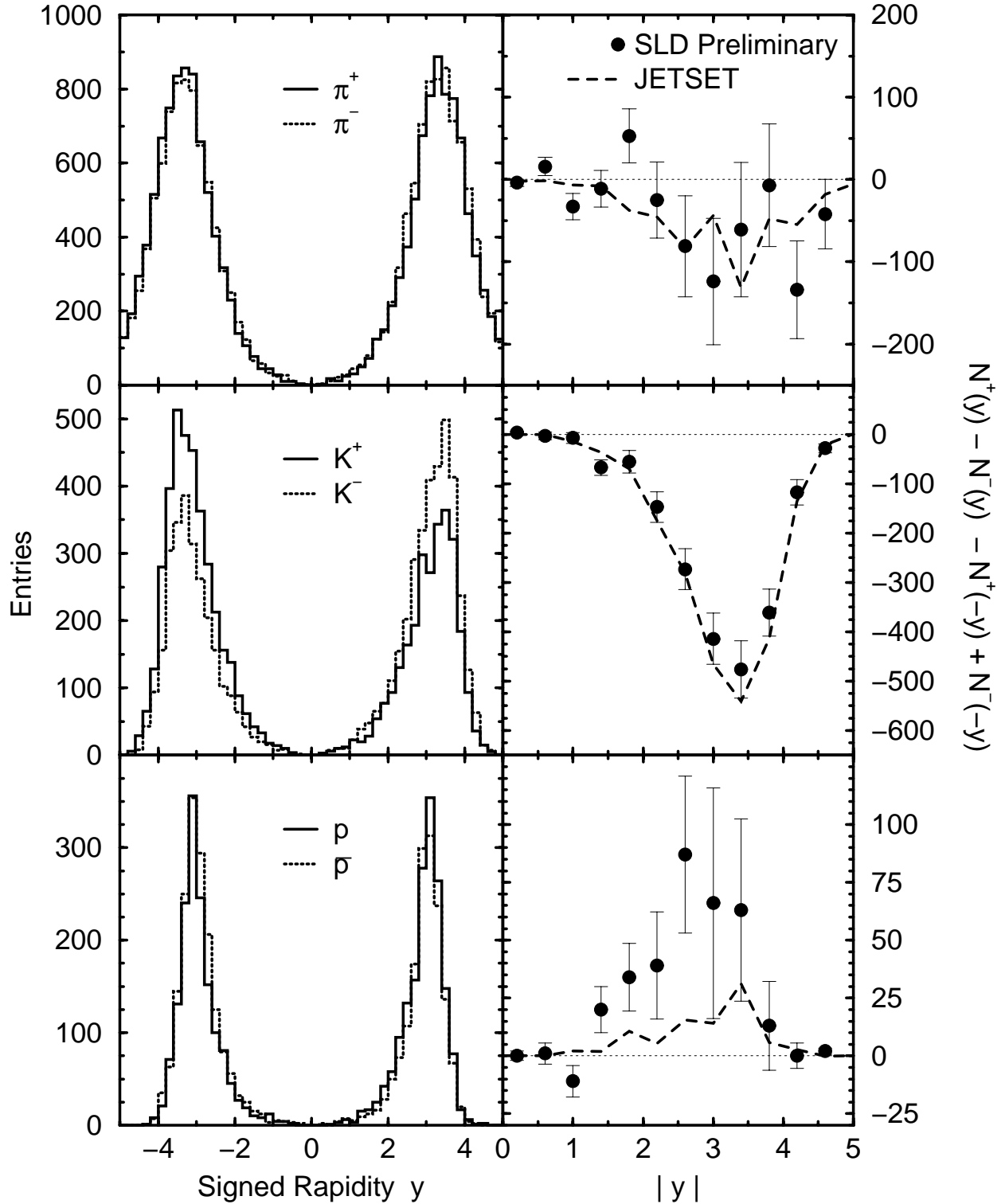


Figure 9: Distributions (left) of the rapidity with respect to the signed thrust axis for positively (histogram) and negatively (dashed histograms) charged identified hadrons with momentum greater than $9 \text{ GeV}/c$. The differences (right) between the asymmetries of each pair of distributions, compared with the prediction of the Monte Carlo simulation.

cle. In fig. 10 we show the distribution of Δy^{+-} for $\pi^+\pi^-$, K^+K^- and $p\bar{p}$ pairs. Asymmetries in these distributions are indications of ordering along the event axis, and the difference between positive and negative sides of these distributions are also shown. The negative difference at high $|\Delta y^{+-}|$ for the K^+K^- pairs can be attributed to the fact that leading kaons are produced predominantly in $s\bar{s}$ events. The positive difference at low $|\Delta y^{+-}|$ for the $p\bar{p}$ pairs indicates that the baryon in an associated baryon-antibaryon pair follows the quark direction more closely than the antibaryon. This could be due to leading baryon production and/or to bryon number ordering along the fragmentation chain. We find a small effect in all six of our momentum bins, however the statistics are not sufficient to distinguish the former possibility, which is expected to be most visible at high momentum, from the latter, which is expected to be independent of momentum. The predictions of the simulation are also shown and are consistent with the data.

For unlike particles, both opposite-charge and same-charge pairs may be of interest. We define the ordered difference as the rapidity of the heavier particle minus that of the lighter particle multiplied by the charge of the heavier particle. That is, $\Delta y^{+-} = y_{K^+} - y_{\pi^-}$ or $y_{\pi^-} - y_{K^+}$, $\Delta y^{++} = y_{K^+} - y_{\pi^+}$, $\Delta y^{--} = y_{\pi^-} - y_{K^-}$, etc. In fig. 11 we show the distributions of Δy^{+-} for opposite-charge pairs of each of the three combinations of unlike particles, as well as the sum of the Δy^{++} and Δy^{--} distributions for the corresponding same-charge pairs. A significant negative asymmetry is observed for πK pairs of both opposite- and same-charge at all Δy , which may simply be due the combination of leading kaons and randomly selected pions. A similar effect in Kp pairs can be attributed leading kaons combined with randomly chosen protons. In this case the asymmetry is negative for opposite-charge pairs and positive for same-charge pairs, as expected given our sign convention. In the case of πp pairs there is a small positive asymmetry for both opposite- and same-charge pairs. The asymmetries predicted by the simulation are also shown and are consistent with the πK and Kp data. No asymmetry is predicted for πp pairs.

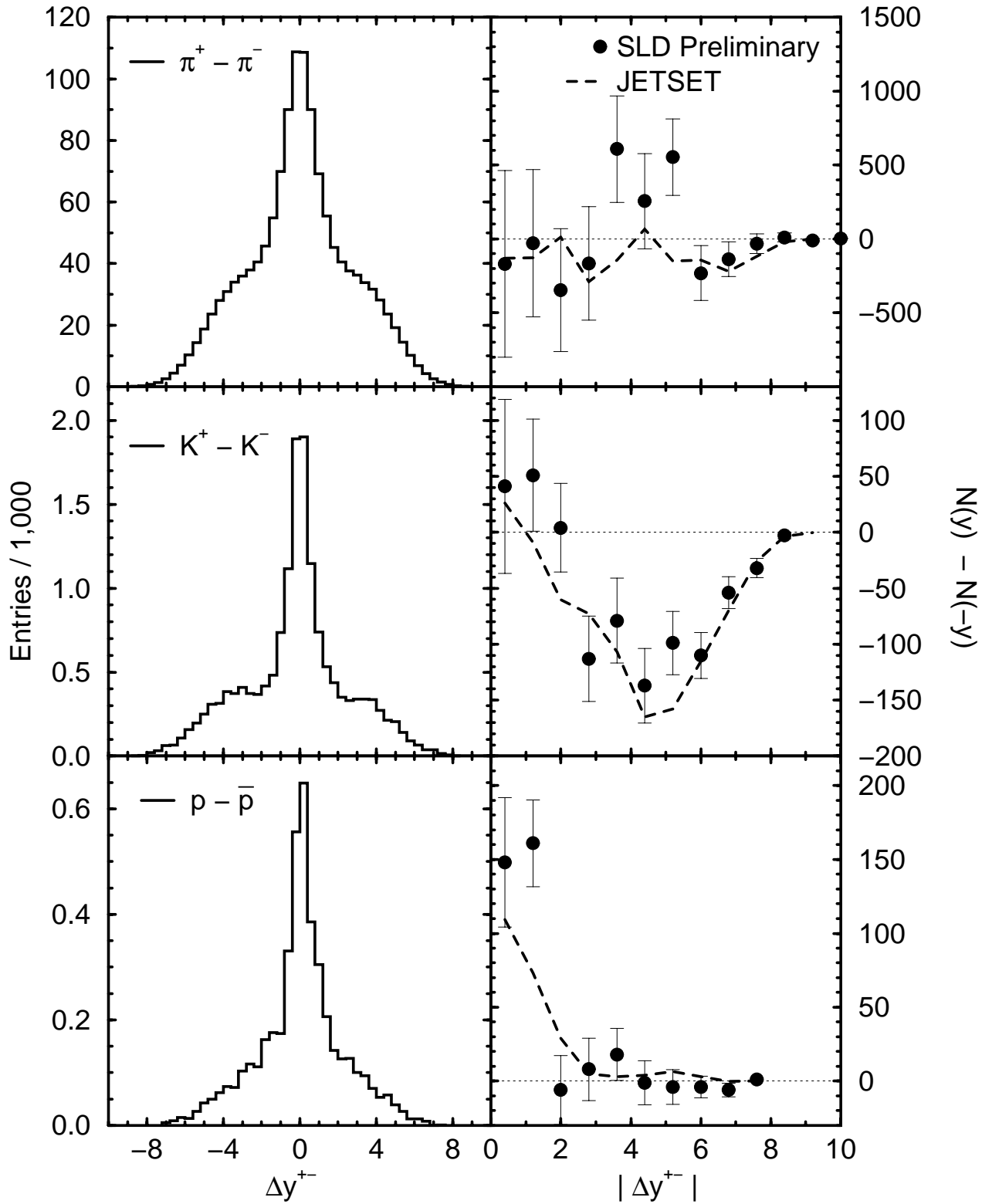


Figure 10: Distributions (left) of the difference between the signed rapidities of positively and negatively charged identified hadrons of the same type. The differences (right) between the right and left sides of the distributions, compared with the prediction of the Monte Carlo simulation.

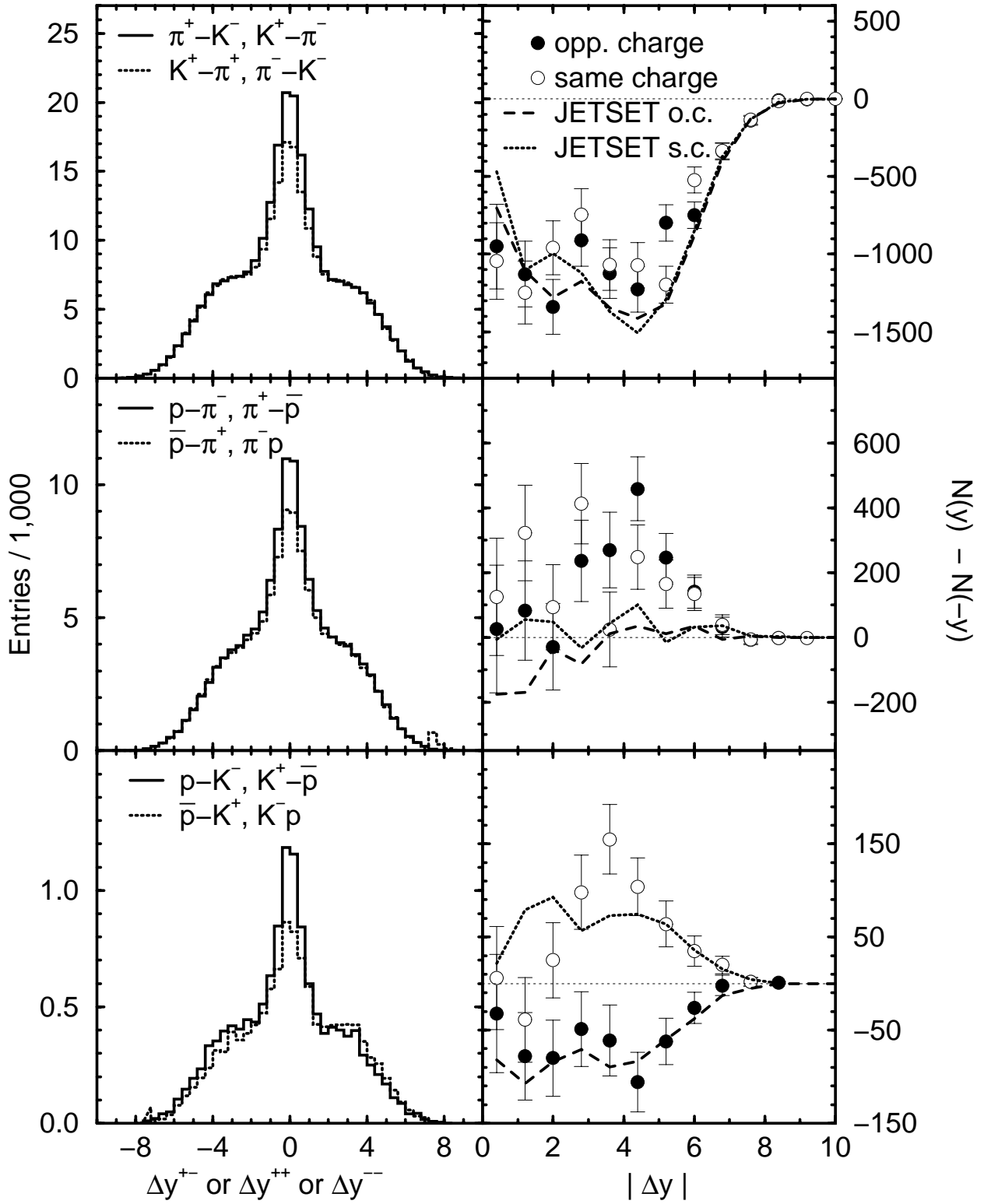


Figure 11: Distributions (left) of the difference between the signed rapidities of positively and negatively charged identified hadrons of different types. The differences (right) between the right and left sides of the distributions, compared with the predictions of the Monte Carlo simulation.

7 Conclusion

We have presented a preliminary study of rapidity differences between pairs of identified charged pions, kaons and protons in light-flavor hadronic Z^0 decays. The SLD Cherenkov Ring Imaging Detector was used to select clean samples of identified charged hadrons, and the Vertex Detector was used to suppress heavy-flavor events.

We observe excesses of opposite-charge over same-charge pairs for all pair types at low values of the absolute rapidity difference, indicating that there is a high degree of local conservation of baryon number, strangeness and electric charge in the fragmentation process. The range of these short-range correlations is found to be independent of momentum but to depend on the types of hadrons forming the pair. The predictions of the JETSET fragmentation model are found to provide a qualitative description of the data, although they fail to describe the shapes of some of the correlations in detail.

We observe a large excess of K^+K^- pairs over same-charge kaon pairs at large values of the absolute rapidity difference, and the effect is larger for higher momenta, as expected from leading kaon production in $s\bar{s}$ events. We observe no such large difference for protons, indicating that events with a leading baryon in one jet, a leading antibaryon in the other and no additional baryons do not contribute significantly to baryon production in e^+e^- annihilations. Considering only tracks with momentum greater than 9 GeV/c, we observe significant long-range correlations between opposite-charge $\pi\pi$, πK and Kp pairs, as well as KK pairs. The simulation provides a good description of the data in general, but predicts smaller long-range πK and Kp correlations than are observed, and predicts a small long-range πp correlation that is not observed.

We have studied distributions of rapidity signed so that positive rapidity corresponds to the quark (rather than antiquark) direction. Differences between signed rapidity distributions for positive and negative hadrons of all three types are observed, giving further evidence for leading production of charged pions kaons and protons. The distribution of the difference between the signed rapidities of K^+ and K^- (p and \bar{p}) shows a large asymmetry at large (small) values of the absolute rapidity difference. The former is a direct indication that the long-range correlated KK pairs are dominated by $s\bar{s}$ events. The latter indicates ordering of baryons along the event axis. Ordered rapidity differences were also studied for other pair types, providing additional tests of

fragmentation models.

Acknowledgements

We thank the personnel of the SLAC accelerator department and the technical staffs of our collaborating institutions for their outstanding efforts on our behalf.

*Work supported by Department of Energy contracts: DE-FG02-91ER40676 (BU), DE-FG03-91ER40618 (UCSB), DE-FG03-92ER40689 (UCSC), DE-FG03-93ER40788 (CSU), DE-FG02-91ER40672 (Colorado), DE-FG02-91ER40677 (Illinois), DE-AC03-76SF00098 (LBL), DE-FG02-92ER40715 (Massachusetts), DE-FC02-94ER40818 (MIT), DE-FG03-96ER40969 (Oregon), DE-AC03-76SF00515 (SLAC), DE-FG05-91ER40627 (Tennessee), DE-FG02-95ER40896 (Wisconsin), DE-FG02-92ER40704 (Yale); National Science Foundation grants: PHY-91-13428 (UCSC), PHY-89-21320 (Columbia), PHY-92-04239 (Cincinnati), PHY-95-10439 (Rutgers), PHY-88-19316 (Vanderbilt), PHY-92-03212 (Washington); The UK Particle Physics and Astronomy Research Council (Brunel, Oxford and RAL); The Istituto Nazionale di Fisica Nucleare of Italy (Bologna, Ferrara, Frascati, Pisa, Padova, Perugia); The Japan-US Cooperative Research Project on High Energy Physics (Nagoya, Tohoku); The Korea Research Foundation (Soongsil, 1997).

References

- [1] TPC Collab., H. Aihara et al., Phys. Rev. Lett. **57** (1986) 3140;
TASSO Collab., R. Brandelik et al., Phys. Lett. **B139** (1984) 126;
ALEPH Collab., D. Buskulic et al., Z. Phys. **C64** (1994) 361;
DELPHI Collab., P. Abreu et al., Phys. Lett. **B416** (1998) 247;
OPAL Collab., P.D. Acton et al., Phys. Lett. **B305** (1993) 415.
- [2] TPC Collab., H. Aihara et al., Phys. Rev. Lett. **53** (1984) 2199;
TASSO Collab., R. Brandelik et al., Phys. Lett. **B100** (1981) 357;
A. Breakstone et al., Z. Phys. **C25** (1984) 21.
- [3] SLD Design Report, SLAC-Report 273 (1984).
- [4] SLD Collaboration: K. Abe et al., Phys. Rev. **D51** (1995) 962.

- [5] M. D. Hildreth et al., Nucl. Instr. Meth. **A367** (1995) 111.
- [6] C.J.S. Damerell et. al., Nucl. Instr. Meth. **A288** (1990) 236.
C.J.S. Damerell et. al., Nucl. Instr. Meth. **A400** (1997) 287.
- [7] K. Abe et al., Nucl. Inst. Meth. **A343** (1994) 74.
- [8] K. Abe et al., SLAC-PUB-7766, submitted to Phys. Rev. D and contributed to this conference.
- [9] S. Brandt et al., Phys. Lett. **12** (1964) 57.
E. Farhi, Phys. Rev. Lett. **39** (1977) 1587.
- [10] D. Axen et al., Nucl. Inst. Meth. **A328** (1993) 472.
- [11] SLD Collab., K. Abe et al., Phys. Rev. **D53** (1996) 1023.
- [12] T. Sjöstrand, Comput. Phys. Commun. **82** (1994) 74.
- [13] P. N. Burrows, Z. Phys. **C41** (1988) 375.
OPAL Collaboration, M.Z. Akrawy et al., Z. Phys. **C47** (1990) 505.
- [14] SLD Collaboration, K. Abe et al., Phys. Rev. Lett. **79** (1997) 590.
- [15] R. Brun et al., Report No. CERN-DD/EE/84-1 (1989).
- [16] SLD Collaboration, K. Abe et al., Phys. Rev. Lett. **74** (1995) 2895.
- [17] K. Abe et al., Nucl. Inst. and Meth. **A371** (1996) 195.
- [18] SLD Collab., K. Abe et al., Phys. Rev. Lett. **78** (1997) 3442.

****List of Authors**

K. Abe,⁽²⁾ K. Abe,⁽¹⁹⁾ T. Abe,⁽²⁷⁾ I.Adam,⁽²⁷⁾ T. Akagi,⁽²⁷⁾ N. J. Allen,⁽⁴⁾
A. Arodzero,⁽²⁰⁾ W.W. Ash,⁽²⁷⁾ D. Aston,⁽²⁷⁾ K.G. Baird,⁽¹⁵⁾ C. Baltay,⁽³⁷⁾
H.R. Band,⁽³⁶⁾ M.B. Barakat,⁽¹⁴⁾ O. Bardou,⁽¹⁷⁾ T.L. Barklow,⁽²⁷⁾ J.M. Bauer,⁽¹⁶⁾
G. Bellodi,⁽²¹⁾ R. Ben-David,⁽³⁷⁾ A.C. Benvenuti,⁽³⁾ G.M. Bilei,⁽²³⁾ D. Bisello,⁽²²⁾
G. Blaylock,⁽¹⁵⁾ J.R. Bogart,⁽²⁷⁾ B. Bolen,⁽¹⁶⁾ G.R. Bower,⁽²⁷⁾ J. E. Brau,⁽²⁰⁾
M. Breidenbach,⁽²⁷⁾ W.M. Bugg,⁽³⁰⁾ D. Burke,⁽²⁷⁾ T.H. Burnett,⁽³⁵⁾ P.N. Burrows,⁽²¹⁾

A. Calcaterra,⁽¹¹⁾ D.O. Caldwell,⁽³²⁾ D. Calloway,⁽²⁷⁾ B. Camanzi,⁽¹⁰⁾
 M. Carpinelli,⁽²⁴⁾ R. Cassell,⁽²⁷⁾ R. Castaldi,⁽²⁴⁾ A. Castro,⁽²²⁾ M. Cavalli-Sforza,⁽³³⁾
 A. Chou,⁽²⁷⁾ E. Church,⁽³⁵⁾ H.O. Cohn,⁽³⁰⁾ J.A. Coller,⁽⁵⁾ M.R. Convery,⁽²⁷⁾
 V. Cook,⁽³⁵⁾ R. Cotton,⁽⁴⁾ R.F. Cowan,⁽¹⁷⁾ D.G. Coyne,⁽³³⁾ G. Crawford,⁽²⁷⁾
 C.J.S. Damerell,⁽²⁵⁾ M. N. Danielson,⁽⁷⁾ M. Daoudi,⁽²⁷⁾ N. de Groot,⁽²⁷⁾
 R. Dell'Orso,⁽²³⁾ P.J. Dervan,⁽⁴⁾ R. de Sangro,⁽¹¹⁾ M. Dima,⁽⁹⁾ A. D'Oliveira,⁽⁶⁾
 D.N. Dong,⁽¹⁷⁾ P.Y.C. Du,⁽³⁰⁾ R. Dubois,⁽²⁷⁾ B.I. Eisenstein,⁽¹²⁾ V. Eschenburg,⁽¹⁶⁾
 E. Etzion,⁽³⁶⁾ S. Fahey,⁽⁷⁾ D. Falciari,⁽¹¹⁾ C. Fan,⁽⁷⁾ J.P. Fernandez,⁽³³⁾ M.J. Fero,⁽¹⁷⁾
 K.Flood,⁽¹⁵⁾ R. Frey,⁽²⁰⁾ T. Gillman,⁽²⁵⁾ G. Gladding,⁽¹²⁾ S. Gonzalez,⁽¹⁷⁾
 E.L. Hart,⁽³⁰⁾ J.L. Harton,⁽⁹⁾ A. Hasan,⁽⁴⁾ K. Hasuko,⁽³¹⁾ S. J. Hedges,⁽⁵⁾
 S.S. Hertzbach,⁽¹⁵⁾ M.D. Hildreth,⁽²⁷⁾ J. Huber,⁽²⁰⁾ M.E. Huffer,⁽²⁷⁾ E.W. Hughes,⁽²⁷⁾
 X.Huynh,⁽²⁷⁾ H. Hwang,⁽²⁰⁾ M. Iwasaki,⁽²⁰⁾ D. J. Jackson,⁽²⁵⁾ P. Jacques,⁽²⁶⁾
 J.A. Jaros,⁽²⁷⁾ Z.Y. Jiang,⁽²⁷⁾ A.S. Johnson,⁽²⁷⁾ J.R. Johnson,⁽³⁶⁾ R.A. Johnson,⁽⁶⁾
 T. Junk,⁽²⁷⁾ R. Kajikawa,⁽¹⁹⁾ M. Kalelkar,⁽²⁶⁾ Y. Kamyshkov,⁽³⁰⁾ H.J. Kang,⁽²⁶⁾
 I. Karliner,⁽¹²⁾ H. Kawahara,⁽²⁷⁾ Y. D. Kim,⁽²⁸⁾ R. King,⁽²⁷⁾ M.E. King,⁽²⁷⁾
 R.R. Kofler,⁽¹⁵⁾ N.M. Krishna,⁽⁷⁾ R.S. Kroeger,⁽¹⁶⁾ M. Langston,⁽²⁰⁾ A. Lath,⁽¹⁷⁾
 D.W.G. Leith,⁽²⁷⁾ V. Lia,⁽¹⁷⁾ C.-J. S. Lin,⁽²⁷⁾ X. Liu,⁽³³⁾ M.X. Liu,⁽³⁷⁾ M. Loreti,⁽²²⁾
 A. Lu,⁽³²⁾ H.L. Lynch,⁽²⁷⁾ J. Ma,⁽³⁵⁾ G. Mancinelli,⁽²⁶⁾ S. Manly,⁽³⁷⁾ G. Mantovani,⁽²³⁾
 T.W. Markiewicz,⁽²⁷⁾ T. Maruyama,⁽²⁷⁾ H. Masuda,⁽²⁷⁾ E. Mazzucato,⁽¹⁰⁾
 A.K. McKemey,⁽⁴⁾ B.T. Meadows,⁽⁶⁾ G. Menegatti,⁽¹⁰⁾ R. Messner,⁽²⁷⁾
 P.M. Mockett,⁽³⁵⁾ K.C. Moffeit,⁽²⁷⁾ T.B. Moore,⁽³⁷⁾ M.Morii,⁽²⁷⁾ D. Muller,⁽²⁷⁾
 V.Murzin,⁽¹⁸⁾ T. Nagamine,⁽³¹⁾ S. Narita,⁽³¹⁾ U. Nauenberg,⁽⁷⁾ H. Neal,⁽²⁷⁾
 M. Nussbaum,⁽⁶⁾ N.Oishi,⁽¹⁹⁾ D. Onoprienko,⁽³⁰⁾ L.S. Osborne,⁽¹⁷⁾ R.S. Panvini,⁽³⁴⁾
 H. Park,⁽²⁰⁾ C. H. Park,⁽²⁹⁾ T.J. Pavel,⁽²⁷⁾ I. Peruzzi,⁽¹¹⁾ M. Piccolo,⁽¹¹⁾
 L. Piemontese,⁽¹⁰⁾ E. Pieroni,⁽²⁴⁾ K.T. Pitts,⁽²⁰⁾ R.J. Plano,⁽²⁶⁾ R. Prepost,⁽³⁶⁾
 C.Y. Prescott,⁽²⁷⁾ G.D. Punkar,⁽²⁷⁾ J. Quigley,⁽¹⁷⁾ B.N. Ratcliff,⁽²⁷⁾ T.W. Reeves,⁽³⁴⁾
 J. Reidy,⁽¹⁶⁾ P.L. Reinertsen,⁽³³⁾ P.E. Rensing,⁽²⁷⁾ L.S. Rochester,⁽²⁷⁾ P.C. Rowson,⁽⁸⁾
 J.J. Russell,⁽²⁷⁾ O.H. Saxton,⁽²⁷⁾ T. Schalk,⁽³³⁾ R.H. Schindler,⁽²⁷⁾ B.A. Schumm,⁽³³⁾
 J. Schwiening,⁽²⁷⁾ S. Sen,⁽³⁷⁾ V.V. Serbo,⁽³⁶⁾ M.H. Shaevitz,⁽⁸⁾ J.T. Shank,⁽⁵⁾
 G. Shapiro,⁽¹³⁾ D.J. Sherden,⁽²⁷⁾ K. D. Shmakov,⁽³⁰⁾ C. Simopoulos,⁽²⁷⁾ N.B. Sinev,⁽²⁰⁾
 S.R. Smith,⁽²⁷⁾ M. B. Smy,⁽⁹⁾ J.A. Snyder,⁽³⁷⁾ H. Staengle,⁽⁹⁾ A. Stahl,⁽²⁷⁾
 P. Stamer,⁽²⁶⁾ R. Steiner,⁽¹⁾ H. Steiner,⁽¹³⁾ M.G. Strauss,⁽¹⁵⁾ D. Su,⁽²⁷⁾ F. Suekane,⁽³¹⁾
 A. Sugiyama,⁽¹⁹⁾ S. Suzuki,⁽¹⁹⁾ M. Swartz,⁽²⁷⁾ A. Szumilo,⁽³⁵⁾ T. Takahashi,⁽²⁷⁾
 F.E. Taylor,⁽¹⁷⁾ J. Thom,⁽²⁷⁾ E. Torrence,⁽¹⁷⁾ N. K. Toumbas,⁽²⁷⁾ A.I. Trandafir,⁽¹⁵⁾
 J.D. Turk,⁽³⁷⁾ T. Usher,⁽²⁷⁾ C. Vannini,⁽²⁴⁾ J. Va'vra,⁽²⁷⁾ E. Vella,⁽²⁷⁾ J.P. Venuti,⁽³⁴⁾
 R. Verdier,⁽¹⁷⁾ P.G. Verdini,⁽²⁴⁾ S.R. Wagner,⁽²⁷⁾ D. L. Wagner,⁽⁷⁾ A.P. Waite,⁽²⁷⁾
 Walston, S.,⁽²⁰⁾ J.Wang,⁽²⁷⁾ C. Ward,⁽⁴⁾ S.J. Watts,⁽⁴⁾ A.W. Weidemann,⁽³⁰⁾
 E. R. Weiss,⁽³⁵⁾ J.S. Whitaker,⁽⁵⁾ S.L. White,⁽³⁰⁾ F.J. Wickens,⁽²⁵⁾ B. Williams,⁽⁷⁾
 D.C. Williams,⁽¹⁷⁾ S.H. Williams,⁽²⁷⁾ S. Willocq,⁽²⁷⁾ R.J. Wilson,⁽⁹⁾
 W.J. Wisniewski,⁽²⁷⁾ J. L. Wittlin,⁽¹⁵⁾ M. Woods,⁽²⁷⁾ G.B. Word,⁽³⁴⁾ T.R. Wright,⁽³⁶⁾
 J. Wyss,⁽²²⁾ R.K. Yamamoto,⁽¹⁷⁾ J.M. Yamartino,⁽¹⁷⁾ X. Yang,⁽²⁰⁾ J. Yashima,⁽³¹⁾
 S.J. Yellin,⁽³²⁾ C.C. Young,⁽²⁷⁾ H. Yuta,⁽²⁾ G. Zapalac,⁽³⁶⁾ R.W. Zdarko,⁽²⁷⁾
 J. Zhou.⁽²⁰⁾

(The SLD Collaboration)

- ⁽¹⁾ *Adelphi University, South Avenue- Garden City, NY 11530,*
⁽²⁾ *Aomori University, 2-3-1 Kohata, Aomori City, 030 Japan,*
⁽³⁾ *INFN Sezione di Bologna, Via Irnerio 46 I-40126 Bologna (Italy),*
⁽⁴⁾ *Brunel University, Uxbridge, Middlesex - UB8 3PH United Kingdom,*
⁽⁵⁾ *Boston University, 590 Commonwealth Ave. - Boston, MA 02215,*
⁽⁶⁾ *University of Cincinnati, Cincinnati, OH 45221,*
⁽⁷⁾ *University of Colorado, Campus Box 390 - Boulder, CO 80309,*
⁽⁸⁾ *Columbia University, Nevis Laboratories P.O.Box 137 - Irvington, NY 10533,*
⁽⁹⁾ *Colorado State University, Ft. Collins, CO 80523,*
⁽¹⁰⁾ *INFN Sezione di Ferrara, Via Paradiso, 12 - I-44100 Ferrara (Italy),*
⁽¹¹⁾ *Lab. Nazionali di Frascati, Casella Postale 13 I-00044 Frascati (Italy),*
⁽¹²⁾ *University of Illinois, 1110 West Green St. Urbana, IL 61801,*
⁽¹³⁾ *Lawrence Berkeley Laboratory, Dept. of Physics 50B-5211 University of California-
Berkeley, CA 94720,*
⁽¹⁴⁾ *Louisiana Technical University, ,*
⁽¹⁵⁾ *University of Massachusetts, Amherst, MA 01003,*
⁽¹⁶⁾ *University of Mississippi, University, MS 38677,*
⁽¹⁷⁾ *Massachusetts Institute of Technology, 77 Massachusetts Avenue Cambridge, MA
02139,*
⁽¹⁸⁾ *Moscow State University, Institute of Nuclear Physics 119899 Moscow Russia,*
⁽¹⁹⁾ *Nagoya University, Nagoya 464 Japan,*
⁽²⁰⁾ *University of Oregon, Department of Physics Eugene, OR 97403,*
⁽²¹⁾ *Oxford University, Oxford, OX1 3RH, United Kingdom,*
⁽²²⁾ *Universita di Padova, Via F. Marzolo, 8 I-35100 Padova (Italy),*
⁽²³⁾ *Universita di Perugia, Sezione INFN, Via A. Pascoli I-06100 Perugia (Italy),*
⁽²⁴⁾ *INFN, Sezione di Pisa, Via Livornese, 582/AS Piero a Grado I-56010 Pisa (Italy),*
⁽²⁵⁾ *Rutherford Appleton Laboratory, Chilton, Didcot - Oxon OX11 0QX United
Kingdom,*
⁽²⁶⁾ *Rutgers University, Serin Physics Labs Piscataway, NJ 08855-0849,*
⁽²⁷⁾ *Stanford Linear Accelerator Center, 2575 Sand Hill Road Menlo Park, CA 94025,*
⁽²⁸⁾ *Sogang University, Ricci Hall Seoul, Korea,*
⁽²⁹⁾ *Soongsil University, Dongjakgu Sangdo 5 dong 1-1 Seoul, Korea 156-743,*
⁽³⁰⁾ *University of Tennessee, 401 A.H. Nielsen Physics Bldg. - Knoxville, Tennessee
37996-1200,*
⁽³¹⁾ *Tohoku University, Bubble Chamber Lab. - Aramaki - Sendai 980 (Japan),*
⁽³²⁾ *U.C. Santa Barbara, 3019 Broida Hall Santa Barbara, CA 93106,*
⁽³³⁾ *U.C. Santa Cruz, Santa Cruz, CA 95064,*
⁽³⁴⁾ *Vanderbilt University, Stevenson Center, Room 5333 P.O.Box 1807, Station B
Nashville, TN 37235,*
⁽³⁵⁾ *University of Washington, Seattle, WA 98105,*
⁽³⁶⁾ *University of Wisconsin, 1150 University Avenue Madison, WI 53706,*
⁽³⁷⁾ *Yale University, 5th Floor Gibbs Lab. - P.O.Box 208121 - New Haven, CT
06520-8121.*

